一、区域地质背景

青藏高原是地球表面规模最大、海拔最高、构造活动性最强的大陆高原，发育元古代、古生代、中生代、新生代不同时期的岩石地层记录和多期区域性构造热事件，经历了长期、复杂的地质演化历史和构造变形过程，逐步形成颇具特色的地壳结构构造和高原地貌格局（吴珍汉等，2003a；Wu et al., 2004）。面积巨大的青藏高原平均海拔高度超过 4500m，被誉为“ 地球第三极 ”，对新生代晚期全球气候环境产生过重大影响；现今仍发育强烈的构造运动和地震活动，是地球表面现今构造活动性最强的大陆构造单元，成为国际地球科学领域公认的大陆动力学野外实验室和地质学家关注的热点研究地区。

青藏高原早古生代、晚古生代、中生代和新生代早期的地质构造与不同时期特提斯古大洋的形成演化、俯冲消减存在密切关系，形成南昆仑缝合带、可可西里缝合带、班公—怒江缝合带、雅鲁藏布江缝合带等构造边界。新生代早中期（始新世—中新世早期），印度大陆发生快速（5-5.5mm/a）北向俯冲，导致青藏地区强烈的挤压构造变形、碰撞造山作用、地壳缩短增厚和青藏高原快速隆升。新生代晚期（中新世中晚期—第四纪），青藏高原构造环境发生显著变化，地壳伸展走滑运动居主导地位，全新世发育 4 条强烈活动断裂、28 条较强烈活动断裂和大量不同方向、不同规模、不同性质的次级活动断层，产生强烈的地震活动，诱发不同类型的地质灾害（吴珍汉等，2004，2005）。

PART 1 TECTONIC SETTING

The Tibetan Plateau is a continent region with the largest scale, the highest elevation and the most intensely tectonic as well as seismic activity. Here exist Proterozoic, Paleozoic, Mesozoic, Cenozoic stratigraphic systems, multiphase of thermo-tectonic events indicating prolonged tectonic evolution, complex structural systems and unique tectono-geomorphic framework (Wu et al., 2003, 2004). And Cenozoic collision between Eurasia and India continental plates not only caused uplift of the Tibetan Plateau over 4500m, but also gave tremendous influence on global climate change and geomorphic features of East Asia.

Tectonics of the Tibetan region in Paleozoic, Mesozoic and Early Cenozoic are closely related to spreading and subduction of Palaeo-Tethys, Meso-Tethys and Neo-Tethys oceanic plates respectively marked by South Kunlun, Hohxil-Jinsha, Bangoin-Nujiang and Indus-Yaluzangbu sutures. Northward subduction of India continental plate at rate of 5-5.5cm/a caused strongly compressional deformation, crust shortening and uplift of the Tibetan Plateau in Eocene-Early Miocene, followed by strike-slip faulting, E-W crust extension and eastward extrusion in Late Miocene-Quaternary and formed 4 very strongly active faults, 28 active faults and many other minor active faults in Holocene, providing favorite tectonic setting for intensely seismic activity and variety of geological hazards along the Golmud-Lhasa Railway (Wu et al., 2004, 2005).

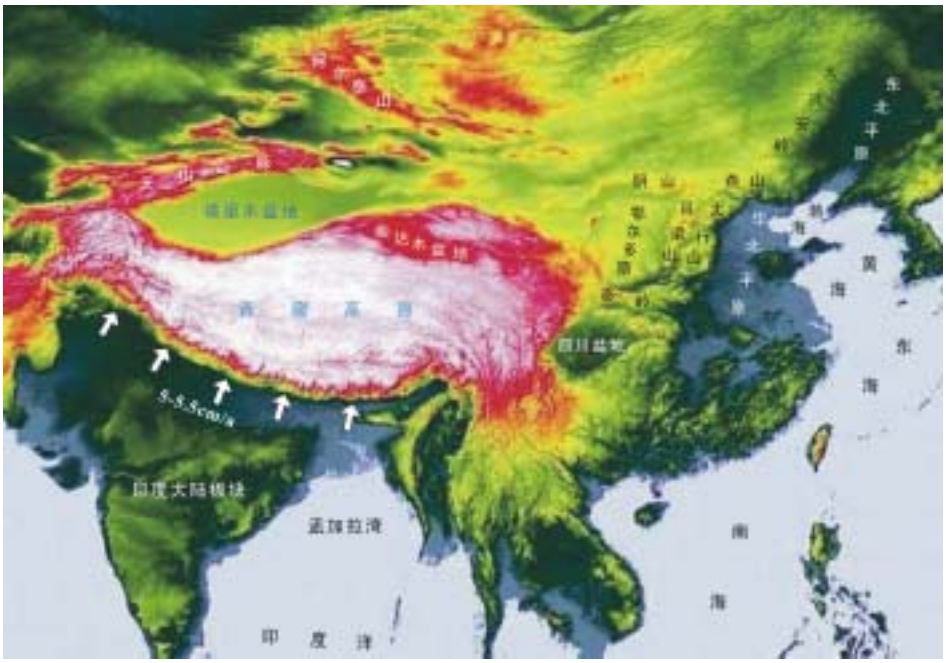


图 1 区域构造地貌图

箭头表示印度大陆板块俯冲方向，5-5.5mm/a 表示新生代晚期印度大陆北向运动速率，白色覆盖区为海拔超过 4500m 的区域。

Fig. 1 Tectono-geomorphic map of the Tibetan Plateau and its adjacent areas. Explanation: arrow shows direction of subduction of India continental plate, 5~5.5mm/a presents northward motion rate of India continental plate since ~ 45-50Ma, white areas indicate plateau region over 4500m.

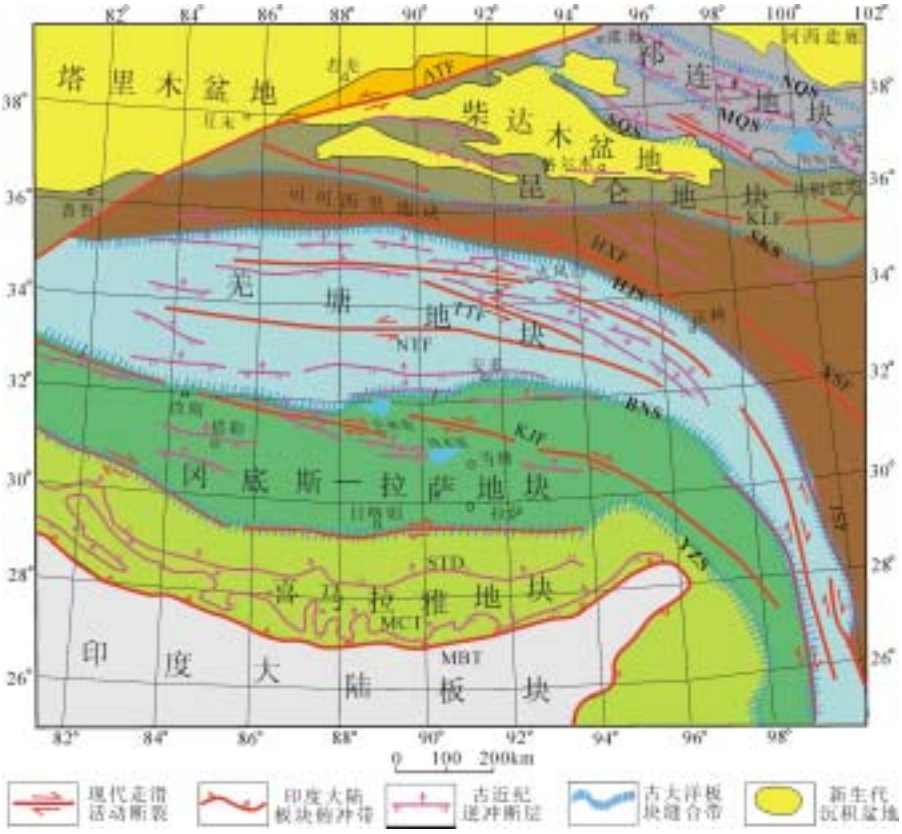


图 2 青藏高原构造单元划分图

NQS-北祁连缝合带；MQS-中祁连缝合带；SQS-南祁连缝合带；SKS-南昆仑缝合带；HJS-可可西里—金沙江缝合带；BNS-班公—怒江缝合带；YZS-雅鲁藏布江缝合带；ATF-阿尔金断裂；KLF-昆仑山断裂；HXF-可可西里断裂；NTF-唐古拉山断裂；XSF-鲜水河断裂；JSF-金沙江断裂；KJF-嘉黎—喀喇昆仑断裂；STD-藏南拆离系；MCT-主中央逆冲断裂；MBT-主边界逆冲断裂。

Fig.2 Sketch map showing division of tectonic units of the Tibetan Plateau. Explanation: NQS-North Qilian suture, MQS-Middle Qilian suture, SQS-South Qilian suture, SKS-South Kunlun suture, HJS-Hohxil-Jinsha suture, BNS-Bangoin-Nujiang suture, YZS-Indus-Yaluzangbu suture. Major boundary faults: ATF-Alkin-Tagh fault, KLF-Kunlun fault, HXF-Hohxil fault, NTF-North Tanggula fault, XSF-Xianshuihe fault, JSF-Jinshajiang fault, KJF-Jiali-Karakorum fault, STD-South Tibet detachment system, MCT-main central thrust, MBT-main boundary thrust.

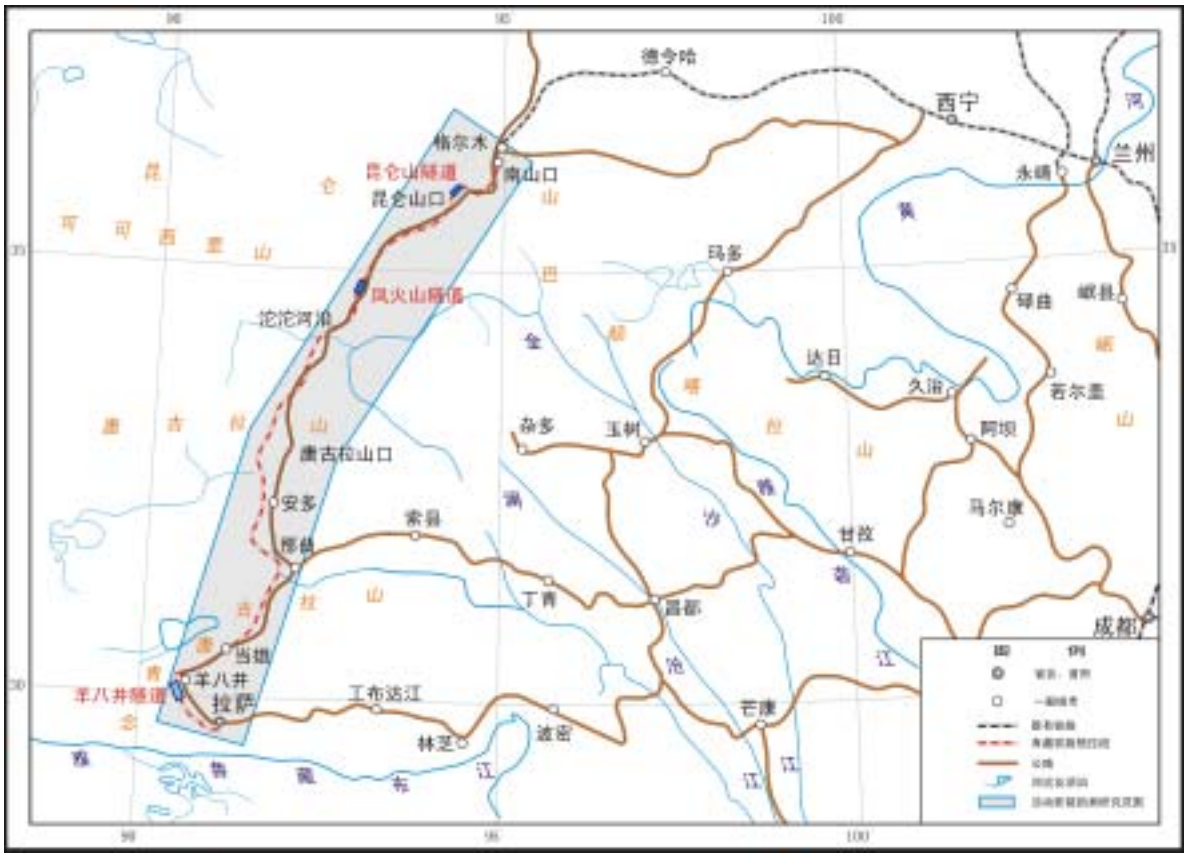


图 3 青藏铁路平面位置图

灰色区域表示 1:10 万路线地质观测范围，铁路两侧各 500m 为 1:2000 活动断层及诱发地质灾害填图范围。兰色标出青藏铁路沿线长度大于 1km 的长隧道，自北向南依次为昆仑山隧道、风火山隧道和羊八井隧道。项目地应力课题组在廖椿庭研究员带领下，在昆仑山隧道北侧、风火山隧道和羊八井隧道分别进行了压磁法地表应测量。发现昆仑山 8.1 级地震前后昆仑山隧道北侧地应力的显著变化，地震前（2001 年 7-8 月）地应力是地震后（2002 年 7-8 月）地应力的 3-4 倍（表 1）。风火山隧道和羊八井隧道的地应力处于正常状态（表 2、3）。

Fig.3 Sketch map showing geographic position of the Golmud-Lhasa Railway. Explanation: gray covers the corridor where 1:100000 geological survey had been finished and 1:2000 mapping of active fault and geological hazard was carried out in 1000m width belt along the Golmud-Lhasa Railway. Blue block marks the position of Kunlunshan, Fenghuoshan and Yangbajain Tunnels from north to south separately where stresses were measured by Liao et al. (2002, 2003). Stresses near Kunlunshan Tunnel decreased evidently after the Ms 8.1 Kunlun Earthquake (Table 1). And stresses keep normal in Fenghuoshan and Yangbajain Tunnels (Table 2, 3).

表 1 昆仑山隧道北侧地应力测量结果一览表

Table 1 Change of stress state in north of Kunlunshan Tunnel before and after the Ms 8.1 Kunlun Earthquake

测点编号 Number	岩 性 Rock Type	深度 Depth (m)	水平最大主应力σ_{max} (Mpa)	水平最小主应力 σ_{min} (Mpa)	最大主应力(σ_{max})方向 Orientation	测量时间 Date of measurement
1	黑云母花岗岩 Biotite granite	18	12.9	12.1	N45°E	2001 年 8 月地震前测量
2	黑云母花岗岩 Biotite granite	18	3.5	3.2	N66°E	2002 年 7 月地震后复测
3	辉长岩 Gabbro	14	6.8	4.4	N58°E	2001 年 8 月地震前测量
4	辉长岩 Gabbro	14	2.2	1.2	N5°W	2002 年 7 月地震后复测

（据 Liao Chunting and Zhang Chunshan et al., 2003）

表 2 风火山隧道及其附近地区地应力测量结果一览表

Table 2 Stress states of the Fenghuoshan Tunnel and its adjacent areas

测点编号 Number	岩 性 Rock Type	深度 Depth (m)	水平最大主应力 σ_{max} (Mpa)	水平最小主应力 σ_{min} (Mpa)	最大主应力(σ_{max})方向
1	粉砂岩 Siltstone	16	5.5	2.9	N84°E
4	泥岩夹中粒砂岩 Mudstone, sandstone	12	4.6	2.8	N61°E
6	泥岩夹细砂岩、粉砂岩 Mudstone, siltstone, sandstone	14	3.6	1.0	N86°E

（据吴满路、廖椿庭等, 2004）

表 3 羊八井隧道群及其周边地区地应力测量结果一览表

Table 3 Stress states of the Yangbajain Tunnel and its adjacent areas

测点编号 Number	岩 性 Rock Type	深度 Depth (m)	水平最大主应力 σ_{max} (Mpa)	水平最小主应力 σ_{min} (Mpa)	最大主应力(σ_{max})方向
1	中细粒黑云二长花岗岩 Biotite granite	13	10.4	8.4	N70°E
2	中细粒黑云二长花岗岩 Biotite granite	12	5.7	2.8	N81°E
3	中粒含角闪二长花岗岩 Amphibolite granite	12	6.6	4.6	N45°E
4	花岗质变余糜棱岩 Granitic mylonite	11	3.3	2.5	N45°E

（据廖椿庭，吴满路等，2002）

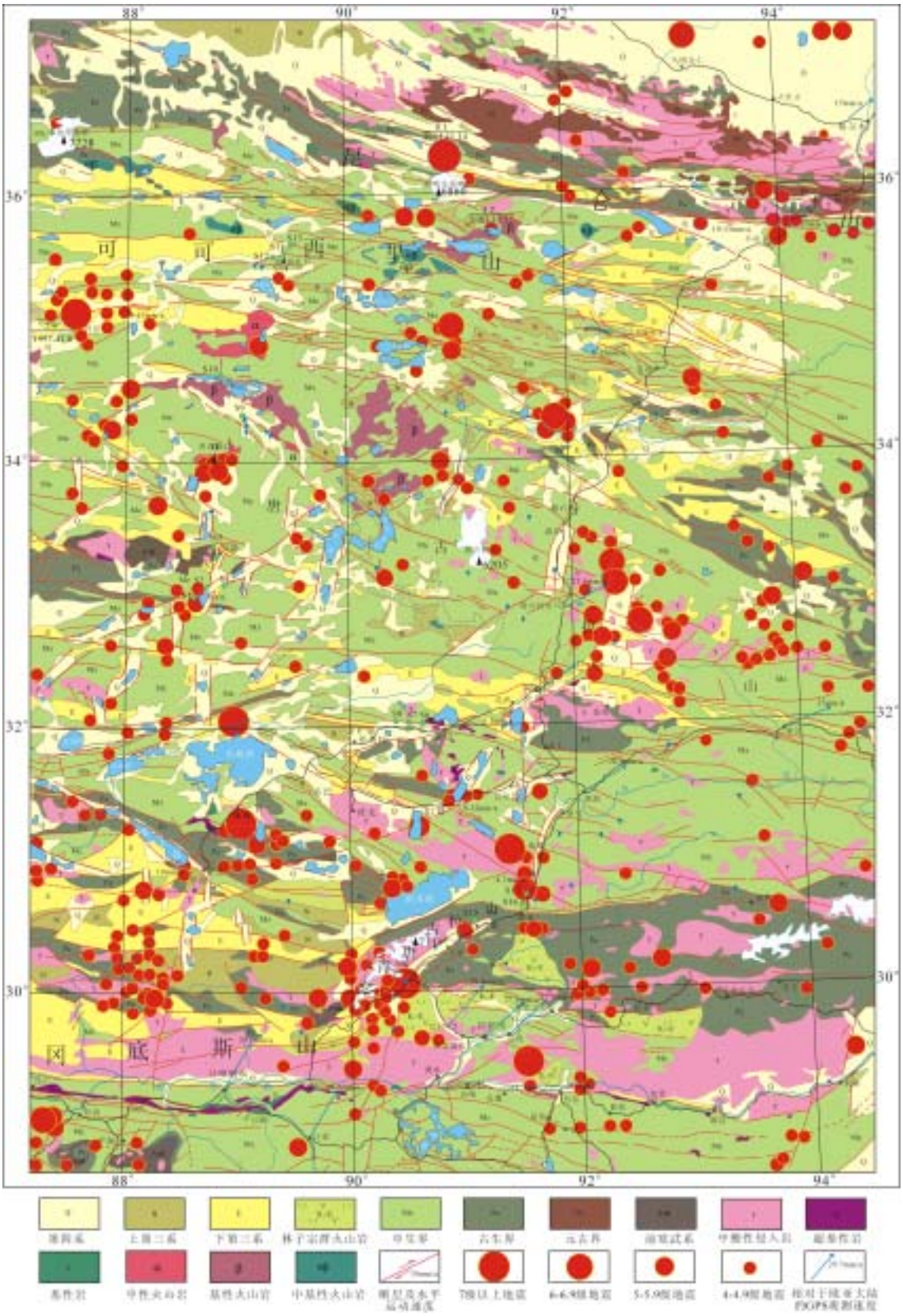


图 4 青藏铁路沿线地质图

（相对于欧亚大陆的运动速度来源于张培震等（2001、2002）GPS 观测资料）

Fig.4 Geological map along the Golmud-Lhasa Railway across the Tibetan Plateau with green arrows indicating absolute velocity relative to Eurasia from GPS data of Zhang et al. (2001, 2002)

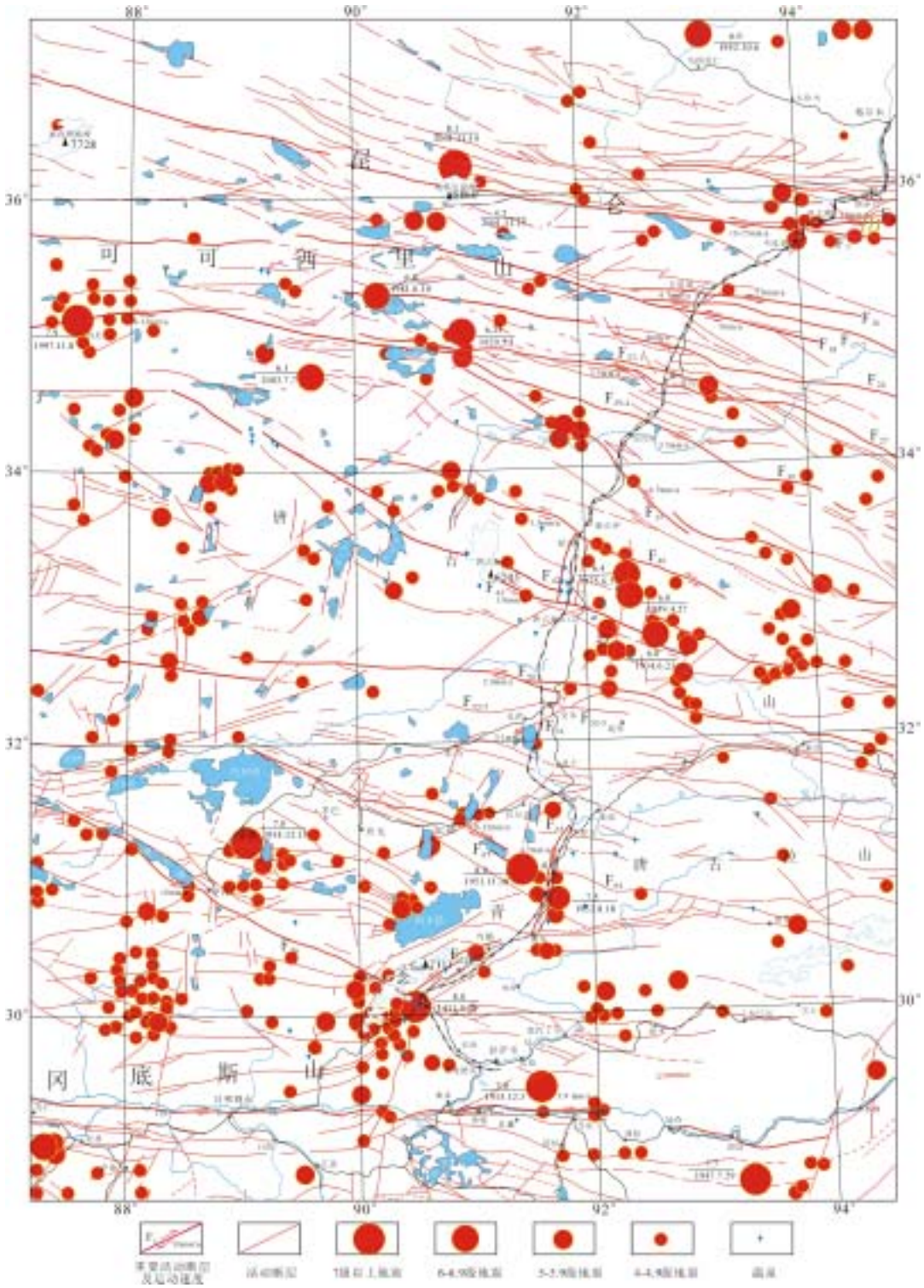


图 5 青藏铁路沿线活动断层与地震分布图

青藏铁路北向南穿越西大滩左旋走滑断裂（F_6）、昆仑山南缘（库赛湖）左旋走滑断裂（F_7）、楚玛尔河活动断裂（F_{15}）、五道梁活动断裂（F_{16}）、可可西里活动断裂（F_{17-2}、F_{18}）、风火山活动断裂（F_{24}）、二道沟盆南活动断裂（F_{27}）、乌丽盆北活动断裂（F_{29-4}）和乌丽山活动断裂（F_{30}）、通天河活动断裂（F_{37}）、雁石坪－木乃山活动断裂（F_{40}）、唐古拉山北活动断裂（F_{43}）、头二九山活动断裂（F_{50}）、崩错右旋走滑断裂（F_{67}）等典型走滑断裂及不冻泉盆地、二道沟盆地、温泉盆地、安多盆地、错那湖盆地、谷露－桑雄盆地、羊八井－当雄盆地等断陷盆地，盆地边缘发育二道沟盆缘活动断裂（F_{26}）、温泉盆西活动断裂（F_{42}）、安多盆北活动断裂（F_{52-5}、F_{52-6}）、安多盆南活动断裂（F_{54}）、谷露－桑雄盆西活动断裂（F_{65}）及念青唐古拉山东南麓当雄－羊八井活动断裂（F_{73}、F_{74}）等伸展活动断裂，大部分断裂运动速率为 1-6mm/a，部分断裂运动速率高达 7-15mm/a。

Fig.5 Active tectonic map along the Golmud-Lhasa Railway across Tibetan Plateau. Explanation: The Golmud-Lhasa Railway extends southward across the Xidatan strike-slip fault (F_6), Hohxil fault (F_{17-2}, F_{18}), Fenghuoshan fault (F_{24}), south Erdaogou fault (F_{27}), North Wuli fault (F_{29-4}), Wuli fault (F_{30}), Tongtianhe fault (F_{37}), Yanshiping-Munaishan fault (F_{40}), North Tanggula fault (F_{43}), Touerjiu fault (F_{50}), Bengco strike-slip fault (F_{67}) etc. and Badongquan basin, Erdaogou basin, Wenqua graben, Amdo basin and Cuonahu, Gulu-sangxiong and Yangbajain-Damxung grabens with normal or oblique slip fault formed in their boundary as marginal fault of Erdaogou basin (F_{26}), West boundary fault of Wenquan graben (F_{42}), north boundary fault of Amdo basin (F_{52-5}, F_{52-6}), south boundary fault of Amdo basin (F_{54}), west boundary fault of Gulu-sangxiong graben (F_{65}) as well as Damxung-Yangbajain active faults in southeast piedmonts of the Nyainqentanglha Mts. (F_{73}, F_{74}). Slip rates of major faults range in 1~6mm/a and that of several faults reach to 7~15mm/a.

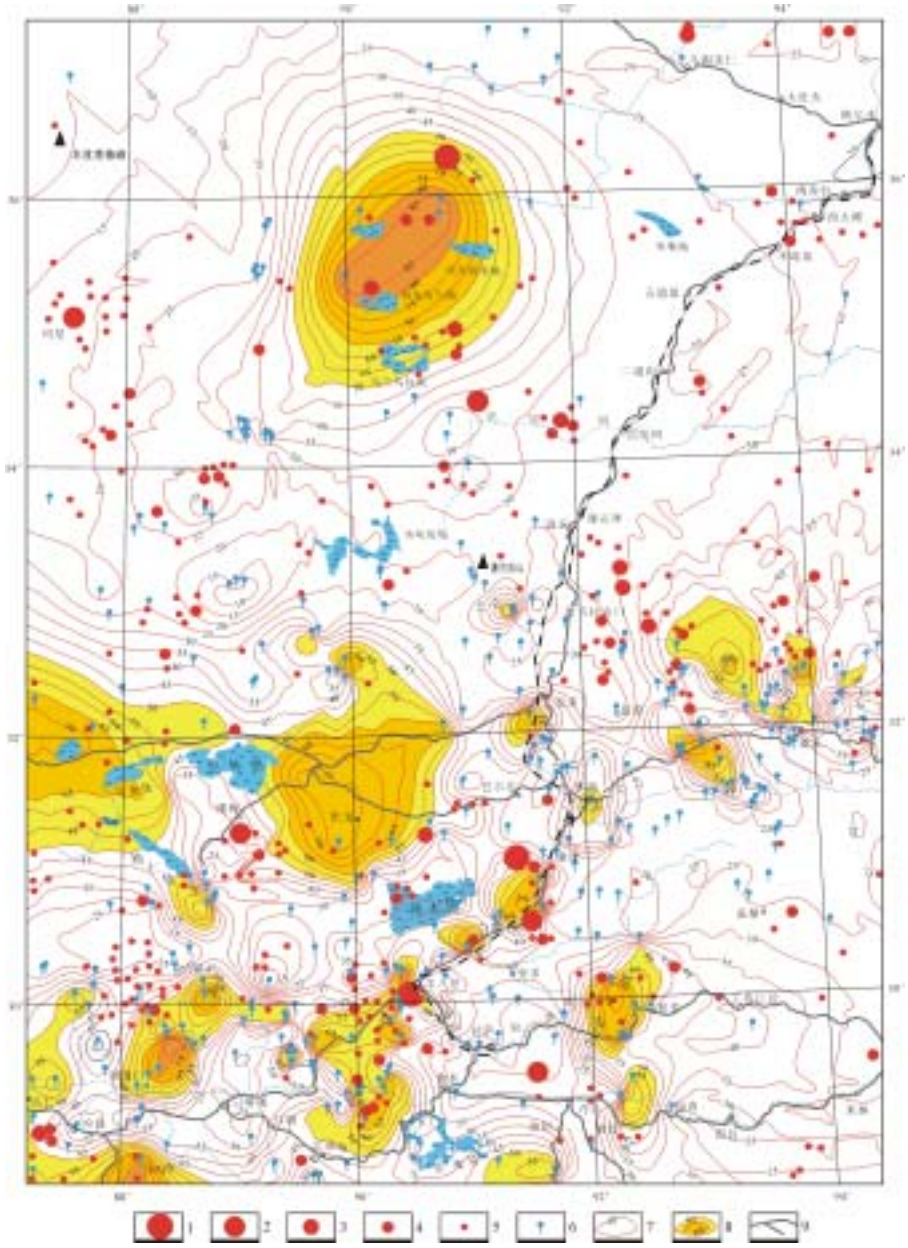


图 6 青藏铁路沿线温泉温度等值线图

1-8.0 级以上地震；2-7.0-7.9 级地震；3-6.0-6.9 级地震；4-5.0-5.9 级地震；5-4.0-4.9 级地震；6-温泉；7-泉口温度等值线（°C）；8-地热异常区；9-干线公路。温泉泉口温度良好地指示地壳热动力状态，Ms≥7 的强烈地震与地壳热动力异常存在良好的对应关系，具有动力学成因联系。

Fig.6 Contour map of hotspring temperature along the Golmud-Lhasa Railway across the Tibetan Plateau indicating geothermal state of upper crust and its links with seismic activity. Explanation: 1-Ms≥8.0 earthquake; 2-Ms 7.0-7.9 earthquake; 3-Ms 6.0-6.9 earthquake; 4-Ms 5.0-5.9 earthquake; 5-Ms 4.0-4.9 earthquake; 6-hotspring; 7-temperature contour (°C) of spring water; 8-anomally geothermal region; 9-highway line.

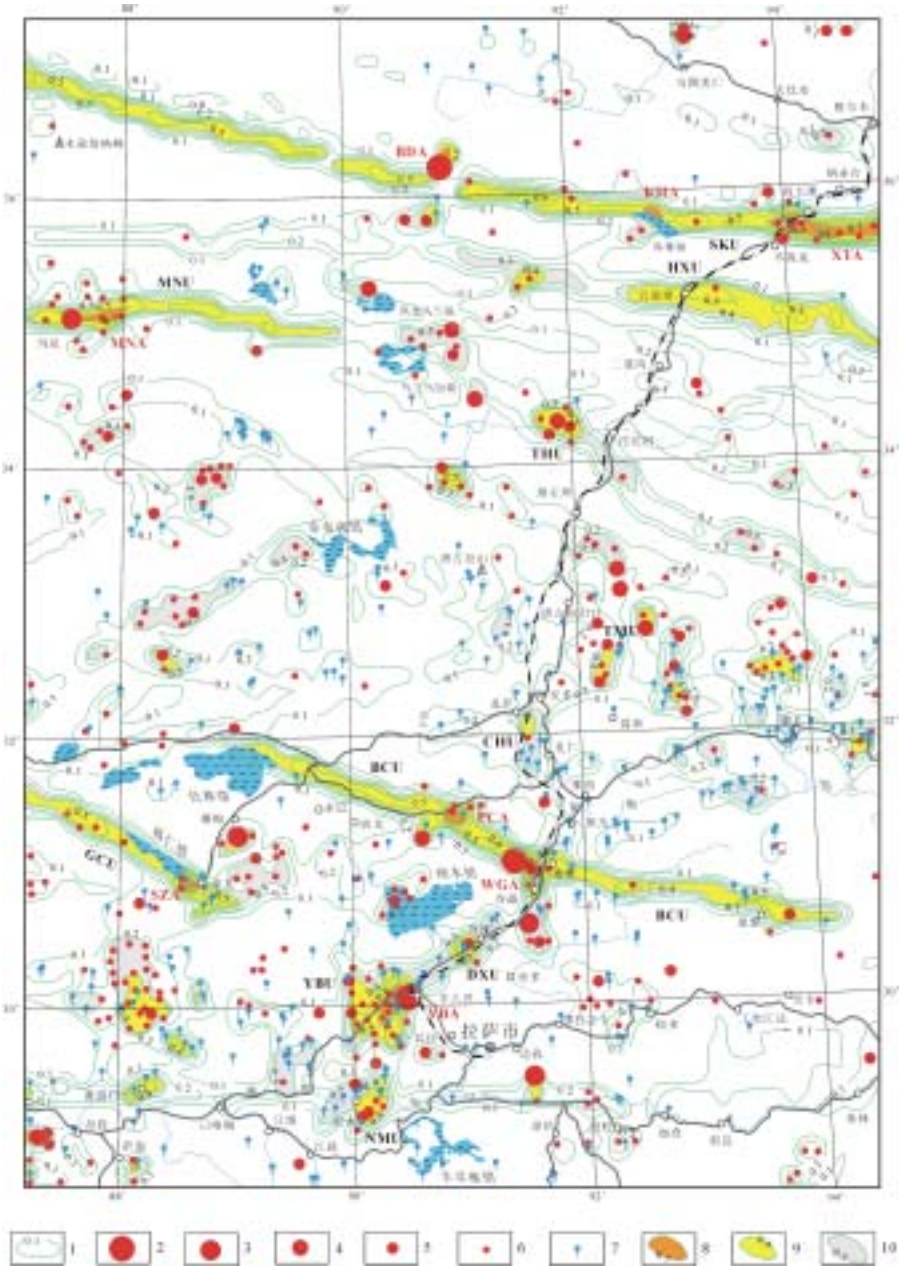


图 7 青藏铁路沿线现今构造活动强度等值线

1-现今构造活动性等值线；2-8.0 级以上地震；3-7.0-7.9 级地震；4-6.0-6.9 级地震；5-5.0-5.9 级地震；6-4.0-4.9 级地震；7-地壳不稳定区；8-温泉；9-现代湖泊。SKU-昆仑山南部不稳定区；HXU-可可西里不稳定区；MNU-玛尼不稳定区；THU-沱沱河不稳定区；TMU-唐古拉山不稳定区；BCU-崩错—嘉黎不稳定区；DXU-当雄不稳定区；YJU-羊八井不稳定区；GCU-格仁错不稳定区。以α（≤1）表示区域构造活动强度，以β（≤1）表示地壳稳定程度，则β=1–α，α=1–β。按 7.6km×7.6km 划分成面积相同的正方形单元。对任一单元 i，现今地壳构造活动强度（α_i）为活动断层运动速率（V_i）、地震震级（M_i）、温泉温度（T_i）和构造应变（ε_i）四个主要参数归一化处理后的加权平均值，$\alpha_i = (V_i/V_{max} + M_i/M_{max} + T_i/T_{max} + \varepsilon_i/\varepsilon_{max})/\ \alpha_{max}$。构造应变充分考虑已有地应力测量和 GPS 观测资料，应用数值模拟方法求出。根据各单元构造活动强度值（α_i），应用克里格等值线绘制软件，制作青藏铁路沿线现今构造活动强度等值线图，揭示现今构造活动区暨地壳不稳定区的空间范围和分布规律。

Fig.7 Isobath map grading intensity of tectonic activity along the Golmud-Lhasa Railway across the Tibetan Plateau. Explanation: 1-isobath contour grading intensity of present tectonic activity; 2-Ms≥8.0 earthquake; 3-Ms 7.0-7.9 earthquake; 4-Ms 6.0-6.9 earthquake; 5-Ms 5.0-5.9 earthquake; 6-Ms 4.0-4.9 earthquake; 7-unstable region; 8-hotspring; 9-present lake. SKU-south Kunlun unstable region; HXU-Hohxil unstable region; MNU-Mani unstable region; THU-Tuotuohe unstable region; TMU-Tanggula unstable region; BCU-Bengco unstable region; DXU-Damxung unstable region; YJU-Yangbajain unstable region; GCU-Gerenco unstable region. Intensity of tectonic activity (α) is graded by 4 major factors including slip rate of active fault (V_i), Richter scale of earthquake (M_i), temperature of hotspring (T_i) and tectonic strain (ε_i) and $\alpha_i = (V_i/V_{max} + M_i/M_{max} + T_i/T_{max} + \varepsilon_i/\varepsilon_{max})/ \alpha_{max}$ for finite unit i as large as 7.6km×7.6km. Tectonic strain came from finite elementary modeling of stress field constrained by data of GPS and stress measurement.